International Journal of ChemTech Research
CODEN (USA): IJCRGG ISSN: 0974-4290
Vol.8, No.7, pp 116-127, 2015

Absorption Spectrum Deconvolution of Zero Air at 1270 nm Band

Muhammad A. AL-Jalali[1], Issam F. Aljghami[2], Yahia M. Mahzia[2]

[1]Physics Department, Faculty of Science, Taif University, Taif, AL-Haweiah, P. O. Box 888,Zip code 21974, Kingdom of Saudi Arabia.
[2]Physics Department, Faculty of Science, Damascus University, Damascus, Syrian Arab Republic.

Emails: aljghami@scs-net.org, yahia.mahzia@gmail.com.

*Corresponding author: aljalaliphys@gmail.com

Abstract: Absorption spectrum to gaseous mixtures of Oxygen –Nitrogen (zero air) were observed under the oxygen (always 20% oxygen in 80% nitrogen) pressure range 1-5 bar and a total pressure range 5-25 bar with temperatures of 298 K, 323 K, 348 k, 373 K.
Data analysis by Viogt deconvolution method indicate to the presence of competition between the two types of spectrum, the first belong to a discrete absorption line around 1268 nm came from O_2 monomer spectrum , and the second from both O_2-O_2 (O_2 dimol) and O_2 - N_2 collision complexes with a continuous absorption band around 1264 nm.
Gaussian width, Lorentzian width, Voigt full width at half-maximum height (Voigt FWHM), absolute area (integrated absorbance) under the spectral line for each line and some physical constants were calculated.
Keywords: O_2 monomer, O_2 dimol, Gaussian width, Lorentzian width, Voigt FWHM, Integrated absorbance. *PACS*: 32.30.Bv, 33.20.Ea, 33.20.-t, 34.50.-s, 34.50.Ez, 51.30. +I . 87.64. km.

Introduction

The absorption spectrum of molecular Oxygen and Nitrogen gas, according to the HITRAN database [1] emphasizes that there is no overlap between the spectrum of oxygen and nitrogen between 1200 -1300 nm wavelengths. It seems that the role of Nitrogen gas only as a collisional mediator in the mixtures of Oxygen-Nitrogen gas.

The Spectral Calculator (www.spectralcalc.com) to the spectra of Nitrogen gas as is shown in figure (1) indicates that it does not have any spectral lines in the region between 1200 to 1330 nm and also ozone(O_3) [2].

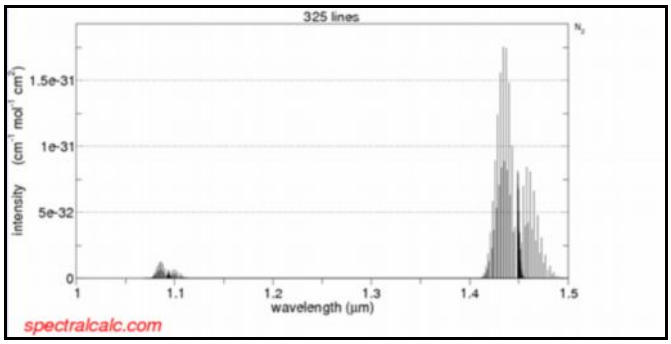

Figure 1. Plot of nitrogen spectrum intensity as function of wavelength in the range of 1 to 1.5 micrometer

Whereas The Spectral Calculator (www.spectralcalc.com) to the spectra of oxygen gas as is shown in figure (2) indicates that it is filled with the spectral lines in the region between 1200 to 1330 nm [3].

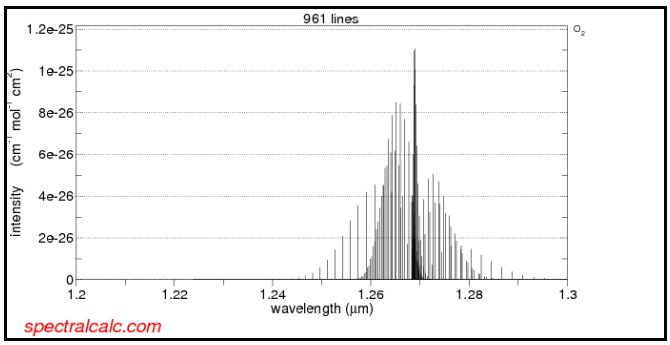

Figure 2. Plot of oxygen spectrum intensity as function of wavelength in the range of 1.2 to 1.3 micrometer

The spectra of oxygen and oxygen-nitrogen mixtures were extensively studied, but the most important researches were by Smith and Newnham et. al. [4-8].

In the near-IR, experimental lines of oxygen-nitrogen mixtures absorption at 1270 nm band show two kinds of absorptions: the first is a discrete lines from individual O_2 molecules (O_2 monomer), and the second is a continuum band, which arise from collision complexes of O_2, such as O_2-O_2 (O_2 dimol(oxygen binary of O_2-O_2)), O_2-N_2. A continuous absorption band is characterized by O_2 dimol and O_2-N_2 spectrum, which is a consequence of collision-induced absorption (CIA) by two O2 or O_2-N_2 in the electrically excited states [9-14].

Monomer oxygen molecule (O_2) is characterized by a zero electric dipole moment, and paramagnetic triplet ground state ${}^3O_2[X\,{}^3\Sigma_g^-(\theta), m_s \quad 0,\pm 1]$ with nearly 5.1 ev dissociation energy (D_e), and shows the rotational structure characteristic of P and R branches. The lowest singlet electronic excitation energies from the O_2 ground state are:

$$a^1\Delta_g(0) \leftarrow X\,{}^3\Sigma_g^-(0) + h\upsilon(1268.4\,nm) \qquad (1)$$

The ground state of O_2-O_2 is ${}^3\Sigma_g^-(\upsilon=0)\,{}^3\Sigma_g^-(\upsilon=0)$, and the first lowest electronic excitation energies from the O_2 dimol ground state due to the following processes:

$${}^3\Sigma_g^-(\upsilon=0)a^1\Delta_g(\upsilon=0) \leftarrow 1264.5nm + {}^3\Sigma_g^-(\upsilon=0)\,{}^3\Sigma_g^-(\upsilon=0) \qquad (2)$$

The aim of this paper is to analyze the experimental results of zero air spectrum at 1270 nm band by Voigt deconvolution method, and find Gaussian, Lorentzian width, Voigt FWHM, integrated absorbance, and get the relation between widths and integrated absorbance as a function of pressure, and some semi empirical expression, which explain some spectral facts.

Theoretical background

Mathematically, the following Beer-Lambert law describes Light-absorption by gas molecules. The ratio of transmitted intensity (I) to incident intensity (I_0) at a given frequency (wavelength λ) is called the transmittance (τ) and given by [4-8]:

$$\tau = \frac{I}{I_0} \quad e^{-\sigma c \ell} = 10^{-A} \Rightarrow A = -\log_{10}\tau \quad \log_{10}\frac{I_0}{I} \quad \sigma c \ell \log e \quad \varepsilon c \ell$$

$$\varepsilon = 0.4343\sigma \Rightarrow \sigma = 2.30225\varepsilon \qquad (3)$$

A is the absorbance at a given wavelength λ , σ is the absorption cross section, and ε is the absorptivity, l is the optical path length, $c = \frac{f\,P}{KT}$ is the concentration, where p is the total gas pressure, f is the absorber gas fraction is the gas constant and T is the gas temperature . If the concentration c is measured in mol.L^{-1}, the absorptivity is called the molar absorptivity.

In most cases, researchers usually use the Napierian absorbance, which is given by:

$$A = \sigma c \ell \qquad (4)$$

Absorbance is an additive function, the total absorbency of a mixture that contains more than one absorbing species (i) at a given wavelength λ is:

$$A = \ell \sum_{i=1}^{n} \sigma_i c_i \qquad (5)$$

It seems that the total cross-section (σ) is the sum of the cross-sections due to absorption, scattering and luminescence …etc. The net absorption cross section for O_2 (m^2 $molecule^{-1}$ or m^2) at the experimental resolution is determined through the following relationship:

$$\sigma_{monomer} = \frac{A}{N_A c \ell} \qquad (6)$$

N_A is the Avogadro constant. For the collision-induced oxygen absorption (O_4) the net binary absorption cross section (m^5 $molecule^{-2}$ (or m^5)) is dependent on the concentration of pairs of O^2 molecules and the absorption cross-section of O2–O2 collision pairs is determined from:

$$\sigma_{dimol} = \frac{A}{(N_A c)^2 \ell} \qquad (7)$$

Broadening of line widths, which contribute to FWHM, may come from natural width according to Heisenberg's uncertainty principle that subject to Lorentzian or natural line. Collisional broadening contributes to the collision line shape by Lorentz distribution function, and the Doppler broadening depends on the Maxwell velocity distribution in a gas, where the Doppler line shape is Gaussian. A Lorentzian always arises from homogeneous broadenings, If two homogeneous mechanisms overlap, the total line shape is another Lorentzian with a bandwidth ($\Gamma_L = \sum_i \Gamma_i^L$), but a Gaussian always arises from Inhomogeneous broadenings, If two inhomogeneous mechanisms overlap, the total line shape is another Gaussian with a bandwidth ($\Gamma_G = \sqrt{\sum_i \Gamma_i^2}$). Doppler broadening most significant at low pressure and high temperature, whereas collision broadening most significant at high Pressure and low temperature, in many sometimes, conditions require consideration of both effects as the convolution of Voigt profile.

Statistical models dealt with gas through collisions, which is recognized from its effective collision time (τ_{eff}) [15-20]:

The relation between effective collision time and full width at half-maximum height (FWHM) was found to be given by:

$$\frac{1}{\tau_{eff}} = n\sigma v \quad \frac{P}{KT}\sigma(8KT/\pi\mu_m)^{\frac{1}{2}} \quad P\sigma(8/\pi\mu_m KT)^{\frac{1}{2}} \qquad (8)$$

Where (P) is the pressure, (n) is the number density of the gas, (σ) is collision cross-section (inelastic collisions are responsible for all the electronic excitation processes), (v) is the average speed of reduced mass (μ_m).

$$\Gamma_L(T,\sigma) \quad \frac{1}{\pi\tau_{eff}} \quad \frac{P\sigma}{\pi}(8/\pi\mu_m KT)^{\frac{1}{2}} \equiv B_{\overline{P}}(T,\sigma)P$$

$$B_P(T,\sigma) \equiv \frac{\partial\Gamma_L}{\partial P} = \frac{\sigma}{\pi}(8/\pi\mu_m KT)^{\frac{1}{2}} \qquad (9)$$

Where $B_P(T,\sigma)$ is well defined the pressure broadening coefficient, and clarify the changes in the collision-induced absorption states, so the change in line width is linear in pressure P (virial equilibrium). In addition, Doppler broadening full width is given by:

$$\Gamma_G(T) \neq 7.7\times10^{-7}\upsilon_c\sqrt{\frac{T}{m}} \qquad [\text{m} = \text{g / moleg/mole of absorber}]$$

$$\upsilon_c = \frac{c}{\lambda_c}, \lambda_c = \text{central wavelength} \qquad (10)$$

At high pressure, real gas inelastic collisions will prevail, and Lorentzian spectral lines will be broadened [21-24].

The Gaussian temperature (Doppler or Gauss effect)-broadened profile and a collision (Lorentz or Lorentz effect)-broadened profile is given as follows [25-27]:

$$I_{Gauss} = I_0(offset) + \frac{A}{\Gamma_G\sqrt{\pi/2}}e^{-2\frac{(\lambda-\lambda_c)^2}{\Gamma_G^2}} \quad (\text{Gaussian intensity profile})$$

$$I_{Lorentz} = I_0(offset) + \frac{2A}{\pi}\frac{\Gamma_L}{4(\lambda-\lambda_c)^2+\Gamma_L^2} \quad (\text{Lorentzian intensity profile}) \qquad (11)$$

Whereas, a Voigt profile, mathematically, is the convolution of the Gaussian and the Lorentzian intensities:

$$I_{Voigt} = I_0(offset) + A\frac{2\ln 2}{\pi^{3/2}}\frac{\Gamma_L}{\Gamma_G^2}\int_{-\infty}^{\infty}\frac{e^{-t^2}}{\left(\sqrt{\ln 2}\frac{\Gamma_L}{\Gamma_G}\right)^2+\left(\sqrt{4\ln 2}\frac{\lambda-\lambda_c}{\Gamma_G}-t\right)^2}dt$$

$$(Voigtian \text{ intensity profile}) \qquad (12)$$

I=absorption intensity, I_0=offset absorption intensity, A=area, Γ_G =Gaussian width, Γ_L = Lorentzian width, $\Gamma_{FWHM} = Voigt\ FWHM$, λ =wavelength, λ_c =central wavelength.

A Voigt profile was developed by Humlíček [28], and gave the equation of the Voigt spectral line width (Voigt FWHM) as follows:

$$\Gamma_{FWHM} \cong 0.5346\Gamma_L + \left(0.2166\Gamma_L^2 + \Gamma_G^2\right)^{\frac{1}{2}} \qquad (13)$$

Where Γ_L Lorentzian width and Γ_G Gaussian width, when Doppler (Gaussian) component is constant and small, Lorentzian distribution will prevail.

Instrumentation

With a brief description, all spectra measurements of oxygen –nitrogen gaseous mixtures were carried out at the spectroscopy laboratory. Absorption spectrum in the NIR was recorded under the mode of baseline corrections in the region of the electromagnet spectrum (1200-1300 nm), by using Cary5000 UV-VIS-NIR spectrophotometer, VARIAN company, equipped with long-pathlength absorption cell (LPAC). The LPAC contains multipass optics in the White cell configuration with a fixed path length of 9.6 m, and its constant volume equal 1.7L. Temperatures range was between 298 to 373 K and pressures of gaseous mixtures between 1 to 5 bars. Experimental measurements was chosen to measure the absorptivity as a function of wavelength in the near infrared region extended between 1200 -1300 nm.

Data analysis and method of spectral line analysis

Spectral measurements on zero air samples (20 % O_2+80 % N_2) was carried out, under the effect of pressure and temperature in the region of the NIR spectrum at 1270 nm band. Origin pro Lab program was used for all data analysis. The Gaussian and Lorentzian width in each spectral line were exactly defined through the deconvolution method of the Voigt profile function.

Table (1) Contains a summary of experimental conditions for measurements of NIR absorption spectra of zero air samples, pressure and temperature values belong to gaseous mixtures of zero air samples (20 % O_2+80 % N_2) which subject to examine at various temperatures.

Table 1. The main information of experimental conditions, where the first column is sample number, the second is Oxygen pressure, the third is Nitrogen pressure, the fourth is the total pressure, and the fifth is temperatures.

Sample	$P(O_2)$ (Bar)	$P(N_2)$ (Bar)	P_{tot} (Bar)	Temperature (K)
1	1	4	5	298
2	1.5	6	7.5	298
3	2	8	10	298
4	2.5	10	12.5	298
5	3	12	15	298
6	3.5	14	17.5	298
7	4	16	20	298
8	4.5	18	22.5	298
9	5	20	25	298
10	1	4	5	323
11	2	8	10	323
12	3	12	15	323
13	4	16	20	323
14	5	20	25	323
15	1	4	5	348
16	2	8	10	348
17	3	12	15	348
18	4	16	20	348
19	5	20	25	348
20	1	4	5	373
21	2	8	10	373
22	3	12	15	373
23	4	16	20	373
24	5	20	25	373

Cary Spectrophotometer was adjusted to the mode of absorbance (dimensionless) as a function of wavelength (nm), Figure (1) shows all spectral lines, which mentioned in the table (1) at various temperatures and pressures.

In all plots , the wavelength at 1264 nm band belong to interaction mechanisms of O_2-O_2 , O_2-N_2 gas where the CIA plays the main role in this band, and the wavelength at 1268 nm belong to O2 gas where a discrete line and ro-vibrational effect plays the main role in this band.

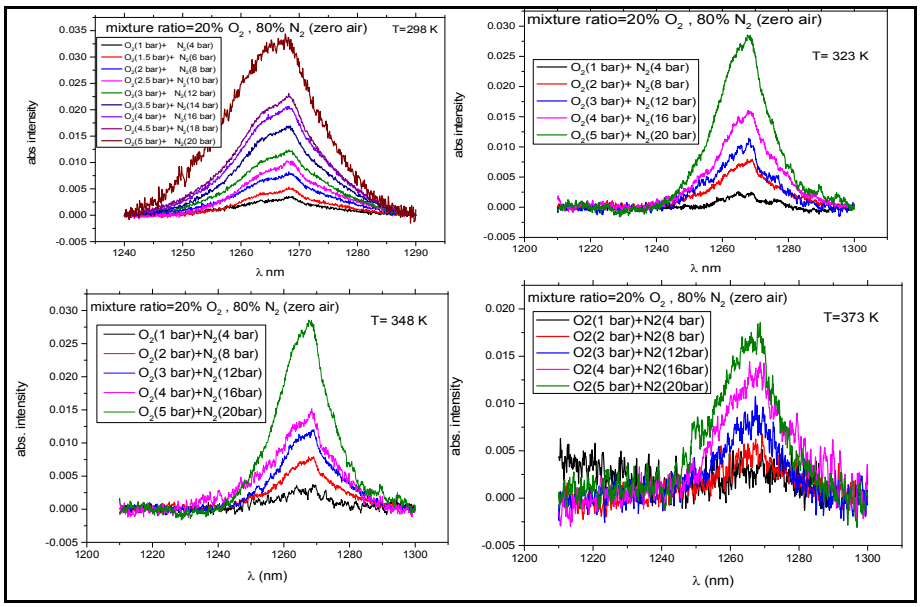

Figure 3. Absorption spectrum for many zero air samples

Method of spectral line analysis:

Each spectral line in figure (3) was subjected to Voigt deconvolution analysis method. For example, Figure (4) shows all **steps were** made to the spectral line belong to (O_2 (1 bar) +N_2 (4bar) to separate O_2 and O_4 absorption line from each other's. Figure (4a) shows the mathematical absolute area (integrated absorbance) under spectral line equal 0.05951. Figure (4b) shows Viogt deconvolution for a spectral line as a line with only one peak, and its area equals 0.07301.

Figure (4c) shows Voigt deconvolution to the spectral line as it has two peaks at central wavelengths belong to 1264 nm and 1268 nm band. Where implicitly each line contains contributions of Gaussian and Lorentzian widths to Voigt full width at half-maximum height.

Figure (4d) shows cumulative (total) Voigt profile with absolute area equals to 0.05964. Figure (4e) shows Voigt profile for 1264 nm band with absolute area equals to 0.0308. Figure (4f) shows Voigt profile for 1268 nm band with absolute area equals to 0.02622. One has to note that the absolute area of the figure (4a or 4d) nearly equal the sum of the absolute area of figures (4e and 4f). Moreover, Viogt area of the figure (4b) nearly equal to the sum of the Voigt area in figure (4e and 4f).

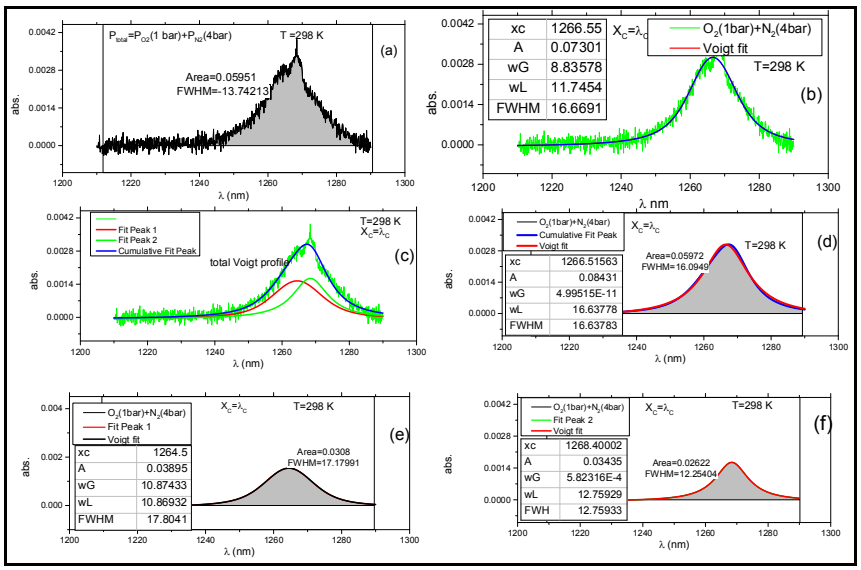

Figure 4. (a-f) The procedure to separate the O_2 monomer and O_2 binary absorbance intensity profile in the 1.27 pm region. See text for a detailed description.

All twenty four spectral lines in figure (3) were subjected to method of spectral line analysis as in figure (4), and all values of absolute area, integrated absorptivity, Lorentzian width, Gaussian width, and Viogt FWHM were tabulated in tables, each table belongs to its special temperature and its band. Because of that, the tables will take a large space, so, they could not be put them in the text, but all tables are available upon request from the authors.

Results and discussion

First of all, Because of parity between the absorbance and absorption cross-section ($A = \sigma c \ell$), all results and values were taken based on the absorbance intensity.

All plots for calculating spectral values according to methods above-mentioned were treated by using the method of least squares to get the "best fit" lines to the data, where the slopes of the plots of all figures are calculated to give some physical coefficients.

So, Gaussian width, Lorentzian width, Voigt FWHM at central wavelengths belong to 1264nm and 1268 nm were plotted as a function of oxygen, nitrogen, and total pressures at 298 k, 323 k ,348 and 373K.

The points of Gaussian and Lorentzian widths were more disorder distribution than Voigt FWHM points, Although, Voigt FWHM values came mathematically from Gaussian and Lorentzian width values(equation 13). In addition, mathematical absolute area (integrated absorbance) values as a function of pressure gave good results to discriminate between O_2 discrete spectral lines and O_2-O_2 continuum spectral lines.

Results could be divided as following:

1. Pressure dependence of widths at 298 K

Figure (5) shows (at 298 K) the conflict between Gauss and Lorentz effect. The values of Gaussian and Lorentzian width seem to be disorder distributed, whereas the Voigt FWHM values appear to be in most order.

Figure (5) indicates to increase of Lorentzian width with pressure, whereas the Gaussian width has the opposite behavior at 1264 nm band, and Voigt FWHM increase with increasing of all kinds of pressures. Linear relations at the figure (5) show the pressure broadening coefficients for various O_2, N_2, O_2+N_2 pressures.

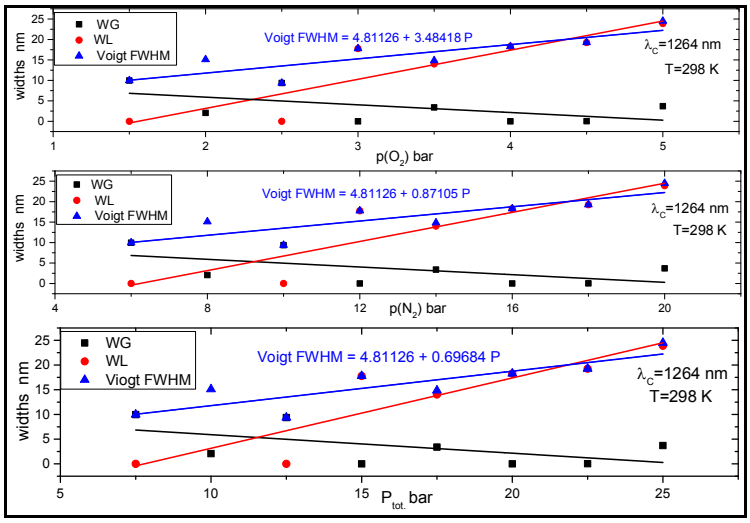

Figure 5. Voigt FWHM, Gaussian, and Lorentzian width as a function of pressure of oxygen, nitrogen and oxygen-nitrogen mixture at 298 K for 1264 nm central wavelength.

In addition, figure (6) at ,also, 298 K shows the behavior at 1268 nm band seems to have inversely values in comparison with 1264 nm band. In other words, at the same time, Lorentzian width increases at 1264 nm band, whereas Lorentzian width decreases at 1268 nm band, and Gaussian width exactly behaves the opposite behavior of the Lorentzian width.

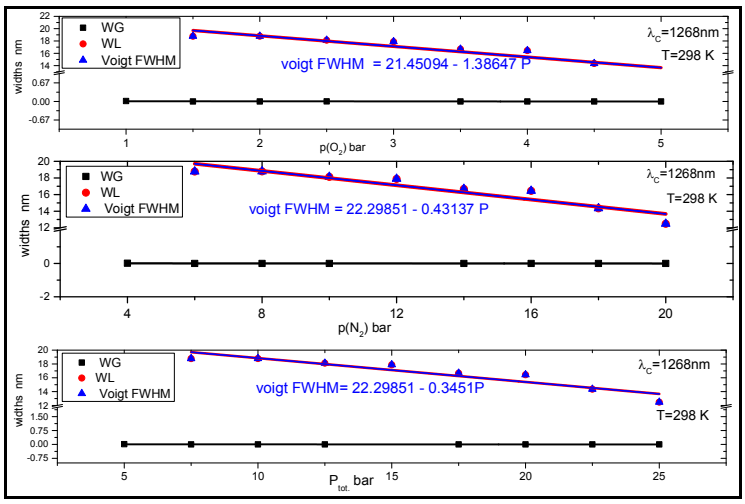

Figure 6. Voigt FWHM, Gaussian, and Lorentzian width as a function of pressure of oxygen, nitrogen and oxygen-nitrogen mixture at 298 K for 1268 nm central wavelength.

2. Pressure dependence of widths at 323 K

Figures (7, 8) at 323 K show the behavior of Voigt FWHM at 1264 nm and 1268 nm, where both Voigt FWHM increase with pressure increasing. Whereas other widths at 1264 nm band seems to have an inversely behavior in comparison with 1268 nm band. In other words, at the same time, Lorentzian width decreases at 1264 nm band with pressure, whereas Lorentzian width increases at 1268 nm band with pressure, and Gaussian width exactly behaves the opposite behavior of the Lorentzian width. Results at 323 K in comparison with the results at 298 K appear to be strange and inconsistent with 298 K results.

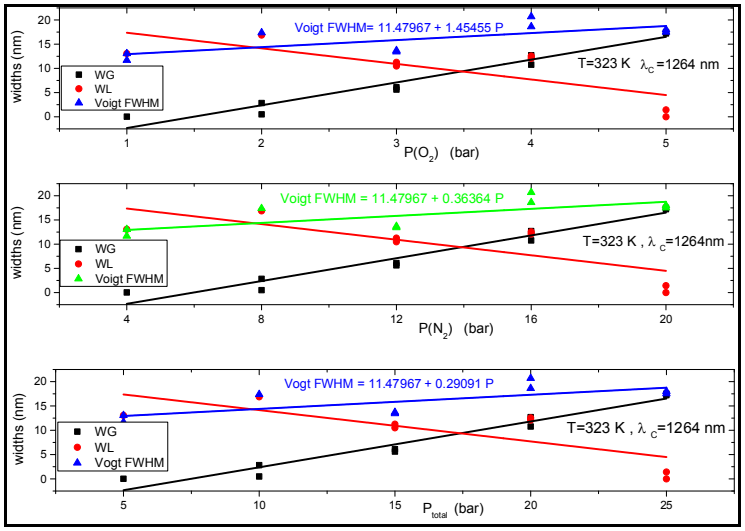

Figure 7. Voigt FWHM, Gaussian, and Lorentzian width as a function of pressure of oxygen, nitrogen and oxygen-nitrogen mixture at 323 K for 1264 nm central wavelength.

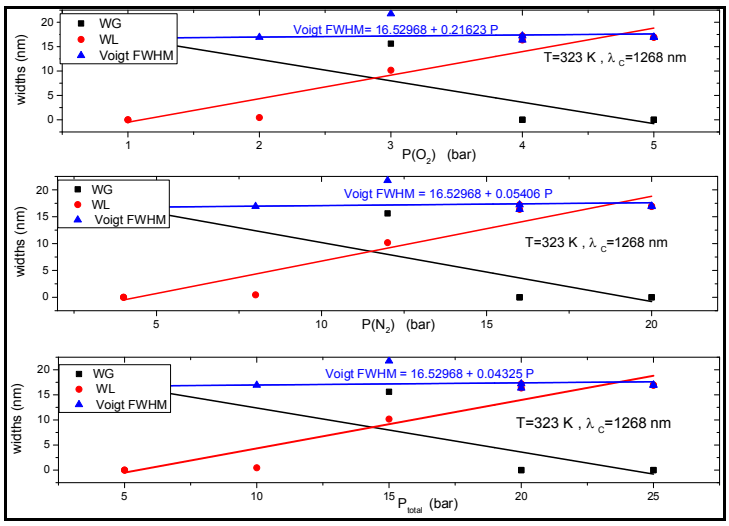

Figure 8. Voigt FWHM, Gaussian, and Lorentzian width as a function of pressure of oxygen, nitrogen and oxygen-nitrogen mixture at 323 K for 1268 nm central wavelength.

3. Pressure dependence of widths at 348 K

Figures (9, 10) show the behavior of widths at 348 K as a function of pressure, it is almost like the widths behavior at 298 k

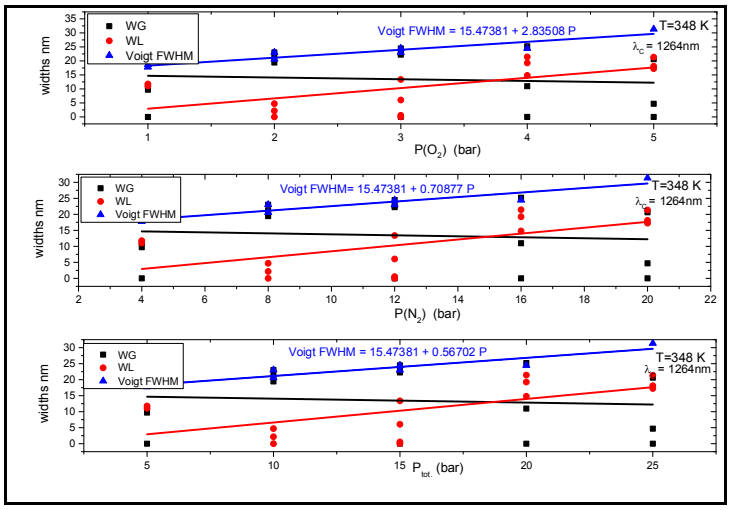

Figure 9. Voigt FWHM, Gaussian, and Lorentzian width as a function of pressure of oxygen, nitrogen and oxygen-nitrogen mixture at 348 K for 1264 nm central wavelength.

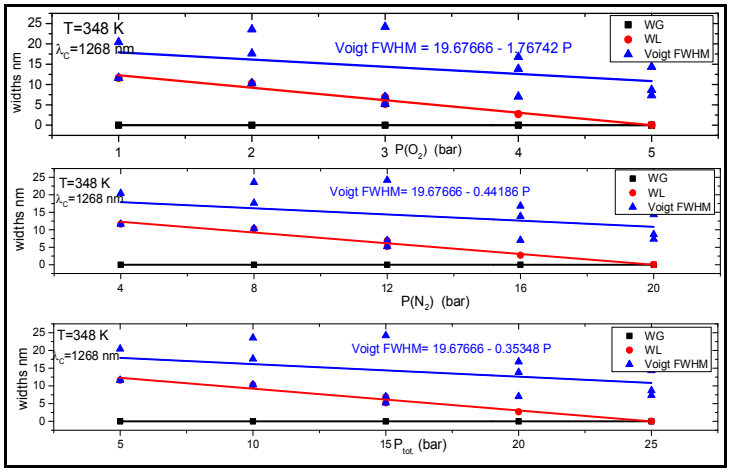

Figure 10. Voigt FWHM, Gaussian, and Lorentzian width as a function of pressure of oxygen, nitrogen and oxygen-nitrogen mixture at 348 K for 1268 nm central wavelength.

4. Pressure dependence of widths at 373 K

At 373 K there are a difficult to get suit fitting between widths and pressures, because the high noisy at 373 k. One could not guess which distribution has to use, figure (11) shows three analysis for each line (a, b, c, d, e) belong to Gauss, Lorentz, and Viogt deconvolution function. The figure shows all subfigures for one peak, at the same time, subject to Gauss, Lorentz and Viogt analysis functions. Where, the last figure (11e) at 25 bar total pressure may be subject to Voigt deconvolution for two peaks, which mean that the two peaks at higher pressure go to reappear.

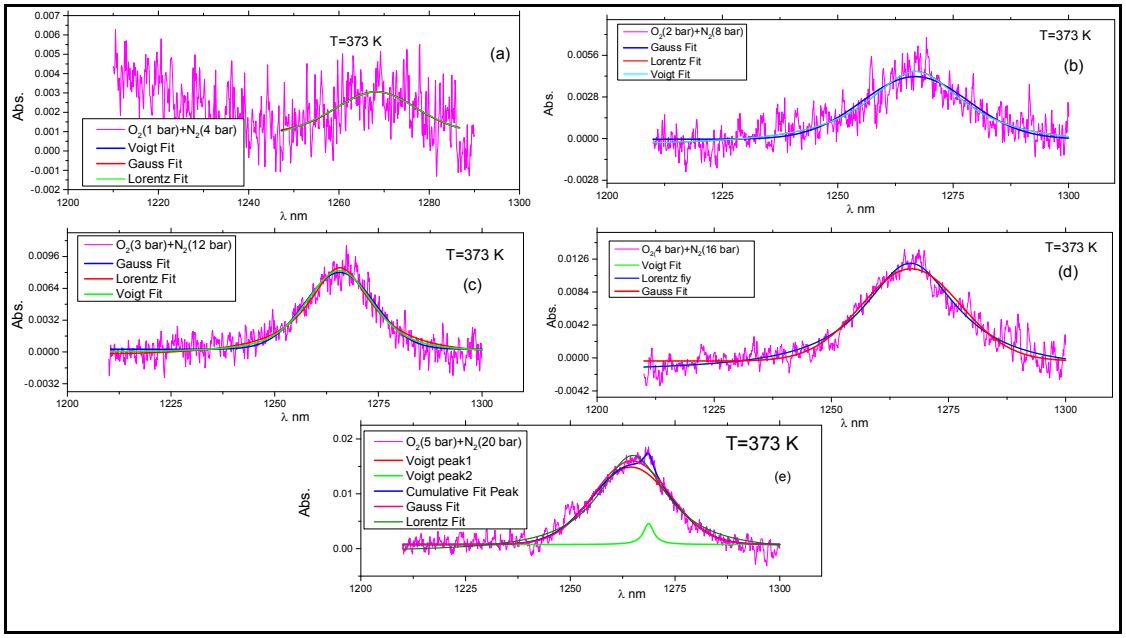

Figure 11. Comparison between the Voigtian, Gaussian and Lorentzian profiles at 373 K.

5. Pressure dependence of integrated absorbance at 298 K, 323K, 348K

Theoretically. The integrated absorbance components have linear (A (1268 nm)) and quadratic (A (1264 nm)) dependence on pressure of O2 (P (O_2)).

Experimentally, figures (12,13,14) indicate to effect of oxygen, nitrogen, and total pressures at integrated absorbance that gave a quadratic pressure dependence of integrated absorbance for 1264 nm band for all temperatures (298 k, 323 k, 348 k), whereas for 1268 nm band only at 348K has a linear pressure dependence of integrated absorbance, but different from others.

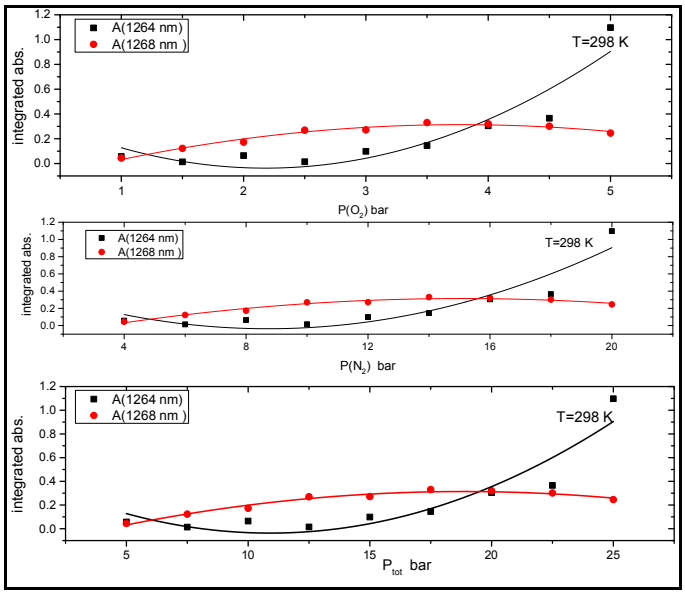

Figure 12. Integrated absorbance as a function of pressures at 298 K

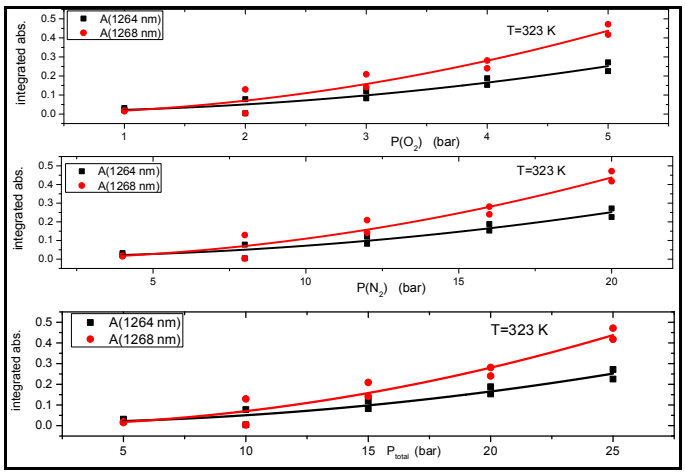

Figure. 13. Integrated absorbance as a function of pressures at 323 K

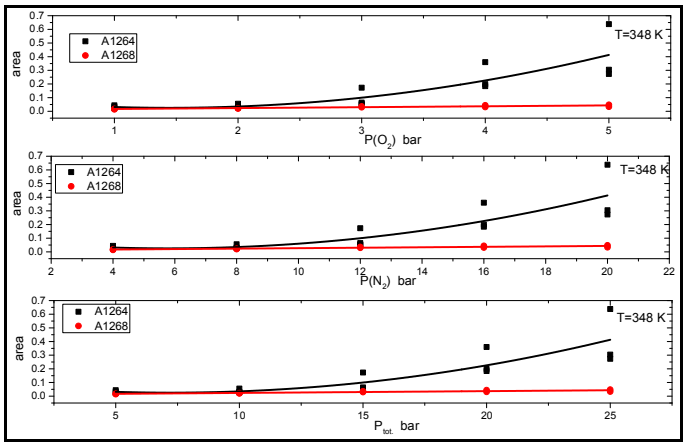

Figure 14. Integrated absorbance as a function of pressures at 348 K

Finally , Figure (12,13,14) show two components of integrated absorbance : one , nearly, with a linear dependence on O_2 ,N_2 partial pressure and total pressure at 1268 nm band , and two with a quadratic pressure dependence for all pressures at 1264 nm band, which agree with theoretical studies.

Conclusion

Voigt deconvolution method to separate two peaks from each other's is a very successful method, because not only separate but also give the values of contribution of Gaussian, Lorentzian widths, and Voigt FWHM for each peak, and the integrated absorbance intensity for two peaks as well.

The widths for zero air confirms that foreign gas (Nitrogen) has a weak effect on the continuum in the 1264 nm region (O_2 dimol), and discrete in the 1268 nm region (O_2 monomer), because Voigt FWHM, Gaussian and Lorentzian widths have the same pressure dependence for all widths although the difference in the O_2, N_2, and total pressures. All widths figures have inversely behaviors between 1264 nm band and 1268 nm band.

The integrated absorbance intensity of continuum absorption at 1264 nm band has quadratic pressure dependence of integrated absorbance for all kinds of partial pressures, which arising from collision-induced or dimol absorption. Whereas for 1268 nm band, which arising from O2 monomer, only at 348K has a linear pressure function with integrated absorbance, but they have a different behavior for others, which need more depth study.

Disorder from thermal and collisional effects was clearly appearing from Gauss and Lorentz effects in all figures.

References

1. Rothman L. S. et.al., The HITRAN 2012 molecular spectroscopic database. Journal of Quantitative Spectroscopy & Radiative Transfer, (2013), 1304–50. doi:10.1016/j.jqsrt.2013.07.002
2. Lofthus A. and Krupenie, P. H., J. Phys. Chem. Ref. Data, 1977, 6, 113–307. http://dx.doi.org/10.1063/1.555546
3. Krupenie P. H., J. Phys. Chem. Ref. Data. 1972, 1423–534. doi:10.1063/1.3253101
4. Newnham D. and Ballard J., J. Geophys. Res., 1998,103, 28801–28815. doi: 10.1029/98JD02799
5. Newman S. M., Orr-Ewing A. J., Newnham D. A. & Ballard J., J. Phys. Chem., 2000, A 104,9467–9480. doi: 10.1021/jp001640r
6. Smith K. M. and Newnham D. A., Journal of geophysical research, 2000, 105, 7383-7396. doi:10.1029/1999JD901171/epdf
7. Smith K. M. & Newnham D. A., Chem. Phys. Lett., 1999, 308, 1–6. doi:10.1016/S0009-2614(99)00584-9
8. Smith K. M., Newnham A. D. & Williams R. G., J. Geophys. Res., 2001, 106, 7541. doi: 10.1029/2000JD900699
9. Maté B., Lugez C. L., Solodov A. M., Fraser G. T. and Lafferty W. J., J. Geophys. Res., 2000, 105, 22,222–225,230. doi: 10.1029/2000JD900295
10. Lemmon E. W., Jacobsen R. T., Penoncello S. G. & Firend D. G., Journal of Physical and Chemical Reference Data, 2000, 29,331–385. http://dx.doi.org/10.1063/1.1285884
11. Sneep M., Ityaksov D., Aben I., Linnartz H. and Ubachs W., Journal of Quantitative Spectroscopy &Radiative Transfer, 2006, 98, 405–424. www.elsevier.com/locate/jqsrt
12. Badger R. M., Wright A. C. and Whitlock R. F., The Journal of Chemical Physics, 1965, 43, 4345. doi: 10.1063/1.1696694
13. Mate' B., Lugez C., Fraser G. T. and Lafferty W. J., journal of geophysical research, 1999, 10430,585-30,590. doi:10.1029/1999JD900824
14. Greenblatt Gary D, Orlando John J, Burkholder James B, and Ravishankara A R, Absorption measurements of oxygen between 330 and 1140 nm, Journal of Geophysical Research, 1990, 95:18577–18582 doi:10.1029/JD095iD11p18577
15. Peach G., Adv. Phys., 1981, 30367–474 doi:10.1080/00018738100101467
16. Jablonski A., Physical Review, 1945, 68, 78-93. doi:10.1103/PhysRev.68.78
17. Loudon R., The Quantum Theory of Light, Second Edition, Chapter2; Oxford University Press, New York, (1983). ISBN 0-19-851155-8.
18. Margenau H., the physical review, 1930, 36, 1782-1790. http://dx.doi.org/10.1103/PhysRev.36.1782
19. Régalia-Jarlot, L., Thomas X., Von der Heyden P. and Barbe A., Journal of Quantitative Spectroscopy and Radiative Transfer, 2005, 91, 121–131. doi:10.1016/j.jqsrt.2004.05.042
20. Devi, V. M., Benner, D. C., Smith M. A. H. and Rinsland C. P., Journal of Quantitative Spectroscopy and Radiative Transfer, 1998, 60, 771–783. doi:10.1016/S0022-4073(98)00081-8
21. Byron Jr., F. W. and Foley H. M., Physical Review, 1964, 134, A625-A637. http://dx.doi.org/10.1103/PhysRev.134.A625
22. Einstein A., "On the Quantum Theory of Radiation", Physikalische Zeitschrift, 18, (1917)121. translated and reprinted by D. ter Haar; The Old Quantum Theory, pages 167-183, Pergamon Press, Oxford(1967). LCCN 66029628
23. Giesen T., Schieder R., Winnewisser G., and Amada K. M. T., Journal of Molecular Spectroscopy, 1992, 153, 406–418. doi:10.1016/0022-2852(92)90485-7
24. Kiehl J. T., and Yamanouchi T., Tellus, 1985, 37B, 1-6. doi:10.1111/j.1600-0889.1985.tb00040.x,
25. Pagnini G., Saxena R.K., A note on the Voigt profile function, arXiv: 0805.2274v1, Submitted to J. Phys. A: Math. Gen, Thu, 15 May (2008).
26. Lether F. G., Wenston P. R., Journal of Computational and Applied Mathematics, 1991, 34, 75–92. doi:10.1016/0377-0427(91)90149-E
27. Yuyan Liu, Jieli Lin, Guangming Huang, Yuanqing Guo, and Chuanxi Duan, Journal of the Optical Society of America B, 2001, 18 , 666-672. doi: 10.1364/JOSAB.18.000666
28. Humlíček J., Journal of Quantitative Spectroscopy and Radiative Transfer, 1982, 27, 437–444. doi:10.1016/0022-4073(82)90078-4.

*****